
HyperTime: Implicit Neural Representation for Time Series

Elizabeth Fons
J. P. Morgan AI Research

Alejandro Sztrajman
University College London

Yousef El-laham
J. P. Morgan AI Research

Alexandros Iosifidis
Aarhus University

Svitlana Vyetrenko
J. P. Morgan AI Research

Abstract

Implicit neural representations (INRs) have recently emerged as a powerful tool that provides an accurate and resolution-independent encoding of data. Their robustness as general approximators has been shown in a wide variety of data sources, with applications on image, sound, and 3D scene representation. However, little attention has been given to leveraging these architectures for the representation and analysis of time series data. In this paper, we analyze the representation of time series using INRs, comparing different activation functions in terms of reconstruction accuracy and training convergence speed. We show how these networks can be leveraged for the imputation of time series, with applications on both univariate and multivariate data. Finally, we propose a hypernetwork architecture that leverages INRs to learn a compressed latent representation of an entire time series dataset. We introduce an FFT-based loss to guide training so that all frequencies are preserved in the time series. We show that this network can be used to encode time series as INRs, and their embeddings can be interpolated to generate new time series from existing ones. We evaluate our generative method by using it for data augmentation, and show that it is competitive against current state-of-the-art approaches for augmentation of time series.

1 Introduction

Modeling time series data has been a key topic of research for many years, constituting a crucial component of applications in a wide variety of areas such as climate modeling, medicine, biology, retail and finance [22]. Traditional methods for time series modeling have relied on parametric models informed by expert knowledge. However, the development of modern machine learning methods has provided purely data-driven techniques to learn temporal relationships. In particular, neural network-based methods have gained popularity in recent times, with applications on a wide range of tasks, such as time series classification [18], clustering [27, 2], segmentation [32, 50], anomaly detection [11, 47, 17], upsampling [30, 6], imputation [24, 25, 9], forecasting [22, 44] and synthesis [1, 48, 21]. In particular, the generation of time series data for augmentation has remained as an open problem, and is currently gaining interest due to the large number of potential applications such as in medical and financial datasets, where data cannot be shared, either for privacy reasons or for proprietary restrictions [20, 21, 3, 12].

In recent years, implicit neural representations (INRs) have gained popularity as an accurate and flexible method to parameterize signals, such as from image, video, audio and 3D scene data [37, 29]. Conventional methods for data encoding often rely on discrete representations, such as data grids, which are limited by their spatial resolution and present inherent discretization artifacts. In contrast, implicit neural representations encode data in terms of continuous functional relationships between

signals, and thus are uncoupled to spatial resolution. In practical terms, INRs provide a new data representation framework that is resolution-independent, with many potential applications on time series data, where irregularly sampled and missing data are common occurrences [14]. However, there are currently no works exploring the suitability of INRs on time series representation and analysis.

In this work, we propose an implicit neural representation for univariate and multivariate time series data. We compare the performance of different activation functions in terms of reconstruction accuracy and training convergence, and we formulate and compare different strategies for data imputation in time series, relying on INRs (Section 4.2). Finally, we combine these representations with a hypernetwork architecture, in order to learn a prior over the space of time series. The training of our hypernetwork takes into account the accurate reconstruction of both the time series signals and their respective power spectra. This motivates us to propose a Fourier-based loss that proves to be crucial in guiding the learning process. The advantage of employing such a Fourier-based loss is that it allows our hypernetwork to preserve all frequencies in the time series representation. In Section 4.3, we leverage the latent embeddings learned by the hypernetwork for the synthesis of new time series by interpolation, and show that our method performs competitively against recent state-of-the-art methods for time series augmentation.

2 Related Work

Implicit Neural Representations INRs (or coordinate-based neural networks) have recently gained popularity in computer vision applications. The usual implementation of INRs consists of a fully-connected neural network (MLP) that maps coordinates (*e.g.* xyz-coordinates) to the corresponding values of the data, essentially encoding their functional relationship in the network. One of the main advantages of this approach for data representation, is that the information is encoded in a continuous/grid-free representation, that provides a built-in non-linear interpolation of the data. This avoids the usual artifacts that arise from discretization, and has been shown to combine flexible and accurate data representation, with high memory efficiency [37, 43]. Whilst INRs have been shown to work on data from diverse sources, such as video, images and audio [37, 10, 33], their recent popularity has been motivated by multiple applications in the representation of 3D scene data, such as 3D geometry [31, 28, 36, 38] and object appearance [29, 41].

In early architectures, INRs showed a lack of accuracy in the encoding of high-frequency details of signals. Mildenhall *et al.* [29] proposed positional encodings to address this issue, and Tancik *et al.* [43] further explored them, showing that by using Fourier-based features in the input layer, the network is able to learn the full spectrum of frequencies from data. Concurrently, Sitzmann *et al.* [37] tackled the encoding of high-frequency data by proposing the use of sinusoidal activation functions (SIREN: Sinusoidal Representation Networks), and Benbarka *et al.* [7] showed the equivalence between Fourier features and single-layer SIRENs. Our INR architecture for time series data (Section 3.1) is based on the SIREN architecture by Sitzmann *et al.* In Section 4.1 we compare the performance of different activation layers, in terms of reconstruction accuracy and training convergence speed, for both univariate and multivariate time series.

Hypernetworks A hypernetwork is a neural network architecture designed to predict the weight values of a secondary neural network, denominated a HypoNetwork [36]. The concept of hypernetwork was formalized by Ha *et al.* [16], drawing inspiration from methods in evolutionary computing [40]. Moreover, while convolutional encoders have been likened to the function of the human visual system [39], the analogy cannot be extended to convolutional decoders, and some authors have argued that hypernetworks much more closely match the behavior of the prefrontal cortex [34]. Hypernetworks have been praised for their expressivity, compression due to weight sharing, and for their fast inference times [39]. They have been leveraged for multiple applications, including few-shot learning [35, 52], continual learning [45] and architecture search [51, 8]. Moreover, in the last two years some works have started to leverage hypernetworks for the training of INRs, enabling the learning of latent encodings of data, while also maintaining the flexible and accurate reconstruction of signals provided by INRs. This approach has been implemented with different hypernetwork architectures, to learn priors over image data [37, 39], 3D scene geometry [23, 38, 36] and material appearance [41]. Tancik *et al.* [42] leverage hypernetworks to speed-up the training of INRs by providing learned initializations of the network weights. Sitzmann *et al.* [37] combine a set encoder

with a hypernetwork decoder to learn a prior over INRs representing image data, and apply it for image in-painting. Our hypernetwork architecture from Section 3 is similar to Sitzmann *et al.*'s, however we learn a prior over the space of time series and leverage it for new data synthesis through interpolation of the learned embeddings. Furthermore, our architecture implements a Fourier-based loss, which we show is crucial for the accurate reconstruction of time series datasets (Section 4.3).

Time Series Generation Realistic time series generation has been previously studied in the literature by using the generative adversarial networks (GANs). In TimeGAN architecture [49], realistic generation of temporal patterns was achieved by jointly optimizing with both supervised and adversarial objectives to learn an embedding space. QuantGAN [46] consists of a generator and discriminator functions represented by temporal convolutional networks, which allows it to synthesize long-range dependencies such as the presence of volatility clusters that are characteristic of financial time series. TimeVAE [13] was recently proposed as a variational autoencoder alternative to GAN-based time series generation. GANs and VAEs are typically used for creating statistical replicas of the training data, and not the distributionally new scenarios needed for data augmentation. More recently, Alaa *et al.* [1] presented Fourier Flows, a normalizing flow model for time series data that leverages the frequency domain representation, currently considered together with TimeGAN as state-of-the-art for time series augmentation.

Data augmentation is well established in computer vision tasks due to the simplicity of label-preserving geometric image transformation techniques, but it is still not widely used for time series with some early work being discussed in the literature [19]. For example, simple augmentation techniques applied to financial price time series such as adding noise or time warping were shown to improve the quality of next day price prediction model. [15]

3 Formulation

In this Section we describe the network architectures that we use to encode time series data (Subsection 3.1), and the hypernetwork architecture (HyperTime) leveraged for prior learning and new data generation (Subsection 3.2).

3.1 Time Series Representation

In Figure 1 we present a diagram of the INR used for univariate time series. The network is composed of fully-connected layers of dimensions $1 \times 60 \times 60 \times 60 \times 1$, with sine activations (SIREN [37]):

$$\phi_i(\mathbf{x}_i) = \sin(\omega_0 \mathbf{W}_i \mathbf{x}_i + \mathbf{b}_i) \tag{1}$$

where ϕ_i corresponds to the i^{th} layer of the network. A general factor ω_0 multiplying the network weights determines the order of magnitude of the frequencies that will be used to encode the signal. Input and output of the INR are uni-dimensional, and correspond to the time coordinate t and the time series evaluation $f(t)$. Training of the network is done in a supervised manner, with MSE loss, and takes less than 10s in a GeForce GTX 1080 Ti GPU. After training, the network encodes a continuous representation of the functional relationship $f(t)$ for a single time series.

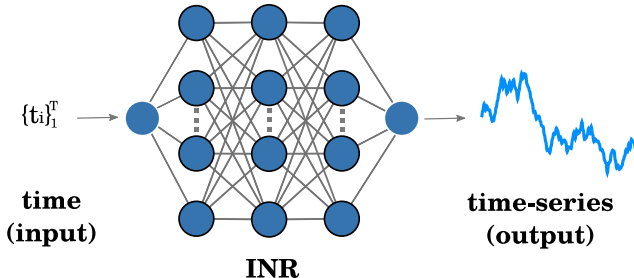


Figure 1: Diagram of the implicit neural representation (INR) for univariate time series. Neurons with a black border use sine activations. The network is composed of fully-connected layers with dimensions $1 \times 60 \times 60 \times 60 \times 1$.

The architecture from Figure 1 can be modified to encode multivariate time series, by simply increasing the number of neurons of the output layer to match the number of channels of the signal. Due to weight-sharing, this adds a potential for data compression of the time series. In addition, the simultaneous encoding of multiple correlated channels can be leveraged for channel imputation, as we will show in Section 4.2.

3.2 Time Series Generation with HyperTime

In Figure 2 we display a diagram of the HyperTime architecture, which allows us to leverage INRs to learn priors over the space of time series. The Set Encoder (green network), composed of SIREN layers [37] with dimensions $2 \times 128 \times 128 \times 40$, takes as input a pair of values, corresponding to the time-coordinate t and the time series signal $f(t)$. Each pair of input values is thus encoded into a full 40-values embedding and fed to the HyperNet decoder (red network), composed of fully-connected layers with ReLU activations (MLP), with dimensions $40 \times 128 \times 7500$. The output of the HyperNet is a one-dimensional 7500-values embedding that contains the network weights of an INR which encodes the time series data from the input. The INR architecture used within HyperTime is the same described in the previous section, and illustrated in Figure 1. Following previous works [36], in order to avoid ambiguities we refer to these predicted INRs as HypoNets.

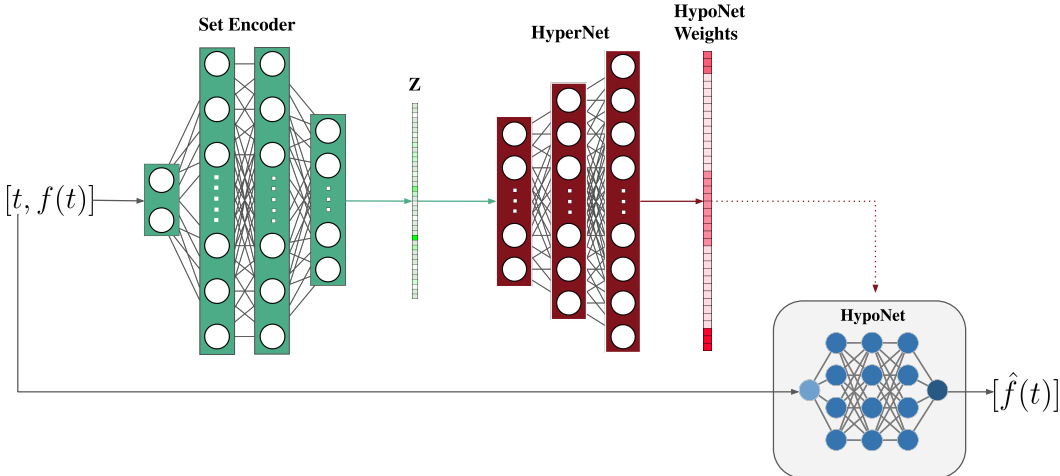


Figure 2: Diagram of HyperTime network architecture. Each pair of time-coordinate t and time series $f(t)$ is encoded as a 40-values embedding Z by the Set Encoder. The HyperNet decoder learns to predict HypoNet weights from the embeddings. During training, the output of the HyperNet is used to build a HypoNet and evaluate it on in the input time-coordinates. The loss is computed as a difference between $f(t)$ and the output of the HypoNet $\hat{f}(t)$.

During the training of HyperTime, we use the weights predicted by the HyperNet decoder to instantiate a HypoNet and evaluate it on the input time-coordinate t , to produce the predicted time series value $\hat{f}(t)$. The entire chain of operations is implemented within the same differentiable pipeline, and hence the training loss can be computed as the difference between the ground truth time series signal $f(t)$ and the value predicted by the HypoNet $\hat{f}(t)$.

After the training of HyperTime, the Set Encoder is able to generate latent embeddings Z for entire time series. In Section 4.3, we show that these embeddings can be interpolated to synthesize new time series signals from known ones, which can be leveraged for data augmentation (see additional material for a pseudo-code of the procedure).

Loss The training of HyperTime is done by optimizing the following loss, which contains an MSE reconstruction term \mathcal{L}_{rec} and two regularization terms $\mathcal{L}_{\text{weights}}$ and $\mathcal{L}_{\text{latent}}$, for the network weights and

the latent embeddings respectively:

$$\mathcal{L} = \underbrace{\frac{1}{N} \sum_{i=1}^N \|f(t_i) - \hat{f}(t_i)\|^2}_{\mathcal{L}_{\text{rec}}} + \lambda_1 \underbrace{\frac{1}{W} \sum_{j=1}^W w_j^2}_{\mathcal{L}_{\text{weights}}} + \lambda_2 \underbrace{\frac{1}{Z} \sum_{k=1}^Z z_k^2}_{\mathcal{L}_{\text{latent}}} + \lambda_3 \mathcal{L}_{\text{FFT}} \quad (2)$$

In addition, we introduce a Fourier-based loss \mathcal{L}_{FFT} that focuses on the accurate reconstruction of the power spectrum of the ground truth signal (see Supplement for more details):

$$\mathcal{L}_{\text{FFT}} = \frac{1}{N} \sum_{i=1}^N \left\| \text{FFT}[f(t)]_i - \text{FFT}[\hat{f}(t)]_i \right\|. \quad (3)$$

In Section 4.3, we show that \mathcal{L}_{FFT} is crucial for the accurate reconstruction of the time series signals.

4 Experiments

4.1 Reconstruction

We start by showing that encoding time series using SIRENS leads to a better reconstruction error than using implicit networks with other activations. We use univariate and multivariate time series datasets from the UCR archive [4].¹ We selected datasets with different characteristics, either short length time series or long, or in the case of the multivariate datasets, with many features (in some cases, more features than time series length). We sample 300 time series (or the maximum number available) from each dataset, train a single SIREN for each time series and calculate the reconstruction error. For comparison we train implicit networks using ReLU, Tanh and Sigmoid activations. As a sample case, we show in Figure 3 the losses (left) and reconstruction plots (right) for one of the univariate datasets (NonInvasiveFetalECGThorax1). Here we observe that sine activations converge much faster, and to lower error values, than other activation functions (for the full set of loss and reconstruction plots, along with a description of each dataset, see additional materials). A summary of results can be found in Table 1, where we observe that the MSE error is at least an order of magnitude lower for sine activations, with respect to other activation layers.

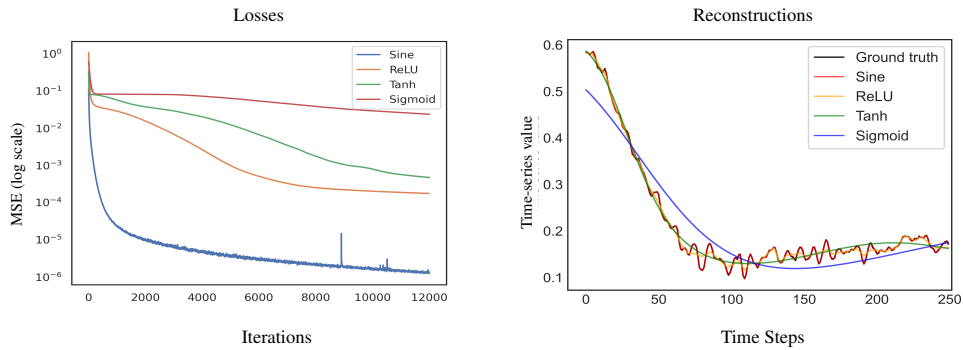


Figure 3: Comparison of implicit networks using different activation functions, MSE loss (*left*) and reconstructed time-series (*right*).

4.2 Imputation

Real world time series data tend to suffer from missing values, in some cases achieving missing rates of up to 90%, making the data difficult to use [14]. Motivated by this, we first use a SIREN trained with the available data points to infer the missing values. Besides fitting a SIREN to the time series, we include a simple regularization term based on a total variation (TV) prior [26]. The TV prior

¹The datasets can be downloaded from the project’s website: www.timeseriesclassification.com [5]

Table 1: Comparison using MSE of implicit networks using different activation functions on different univariate and multivariate time series from the UCR dataset.

	Sine	ReLU	Tanh	Sigmoid
<i>Univariate</i>				
Crop	5.1e-06	5.4e-03	2.8e-02	5.1e-01
NonInvasiveFetalECGThorax1	2.3e-05	2.8e-02	5.7e-02	8.1e-02
PhalangesOutlinesCorrect	7.5e-06	1.9e-02	1.4e-01	3.3e-01
FordA	9.2e-06	1.4e-01	1.5e-01	1.5e-01
<i>Multivariate</i>				
Cricket	1.6e-04	4.2e-03	5.1e-03	1.6e-02
DuckDuckGeese	9.1e-05	8.0e-04	8.7e-04	9.1e-04
MotorImagery	1.7e-03	1.1e-02	1.1e-02	1.8e-02
PhonemeSpectra	1.1e-06	6.0e-03	1.6e-02	1.8e-02

samples random points $t_i \in [-1, 1]$ from the available points of the time series (those that do not have missing values) and the regularization consists of the L1 norm on the gradient

$$p_{TV} = \frac{1}{N} \sum_{i=1}^N |\nabla \Phi_{\theta}(t_i)|.$$

We compare this approach with common time series imputation methods, *mean*, that fills missing values with the average, *kNN*, *cubic spline* and *linear*. We are not solely interested in the reconstruction error, but also in the accurate and smooth reproduction of the Fourier spectrum composition of the original time series. Therefore, we evaluate both the MSE of the time series reconstruction, and the MAE between the Fourier spectra of ground truth and reconstructed, that we name Fourier Error (FFTE).

Table 2 shows the comparison of SIREN with and without prior with the classical methods using different ratios of missing values. We can see that the reconstruction error from baseline methods tends to be low, although when we compare the spectrum through FFTE, we can see that the lowest errors are achieved by SIREN, except when we have a fraction of missing values of 90%, where in small time series such as Crop or Phalanges, that have less than 100 time steps, both reconstruction error and FFTE are poor. With regard to adding a prior over the gradient, we can see that for very short time series such as Crop and Phalanges (which are 46 and 80 time steps of length, respectively), the prior improves the reconstruction error when compared to SIREN without a prior, and this is also the case for FFTE. Figure 4 shows the comparison of SIREN, SIREN plus TV prior and Linear for a randomly selected time series from the NonInvasiveFetalECGThorax1 (NonInv) dataset with 70% of data points missing (the plot is zoomed in a segment of 250 timesteps to highlight the imputation characteristics). We can see that the linear imputation is not smooth, so it's not a good representation of the series, while SIREN is smooth but tends to have higher deviations from the series. SIREN plus the TV prior is a good compromise between maintaining the smoothness of the series while also deviating less from the ground truth.

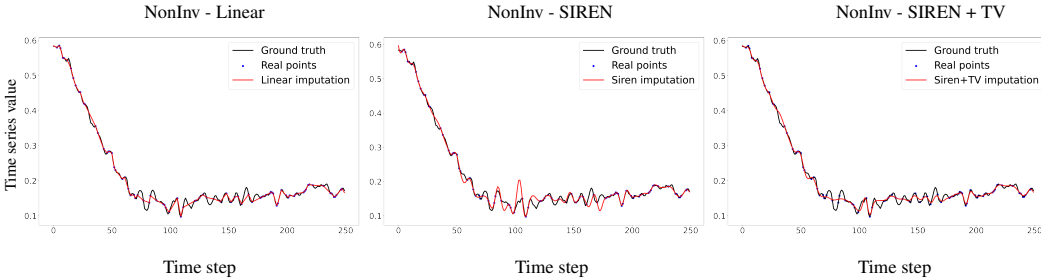


Figure 4: Comparison of imputation methods, zoomed in 250 time steps for the NonInv dataset, with 70% of missing values.

Table 2: Comparison of implicit neural representations (INRs) with classical imputation methods using different fractions of missing values. Each method shows the MSE reconstruction errors and the Fourier reconstruction errors.

	SIREN		SIREN_TV		Mean		kNN		Cubic Spline		Linear		
	MSE	FFTE	MSE	FFTE	MSE	FFTE	MSE	FFTE	MSE	FFTE	MSE	FFTE	
Crop	0.0	5.5e-07	0.00	1.7e-06	0.01	-	-	-	-	-	-	-	
	0.1	6.5e-03	0.43	1.2e-03	0.18	1.7e-02	3.01	1.7e-02	3.03	6.7e-07	2.25	2.2e-06	2.25
	0.5	1.2e-01	1.80	1.3e-02	0.63	1.7e-02	3.02	1.6e-02	2.97	8.3e-05	2.25	7.6e-05	2.25
	0.7	2.9e-01	2.52	3.8e-02	0.95	1.7e-02	3.03	1.7e-02	3.03	9.5e-03	2.25	8.6e-04	2.24
	0.9	5.4e-01	2.74	3.5e-01	2.02	1.7e-02	3.02	1.7e-02	3.00	1.1e+02	2.49	1.6e-02	2.24
NonInv	0.0	1.5e-06	0.02	3.5e-06	0.04	-	-	-	-	-	-	-	
	0.1	2.1e-06	0.03	4.7e-06	0.04	1.7e-02	3.00	1.6e-02	2.97	3.5e-07	2.25	2.2e-06	2.25
	0.5	9.2e-05	0.15	7.6e-05	0.14	1.7e-02	3.00	1.7e-02	3.02	1.1e-04	2.25	1.1e-04	2.25
	0.7	1.2e-03	0.46	1.3e-03	0.45	1.7e-02	2.99	1.7e-02	2.99	1.7e-02	2.25	6.9e-04	2.24
	0.9	1.5e-02	1.40	1.6e-02	1.55	1.6e-02	2.98	1.6e-02	2.97	2.8e-01	2.27	1.8e-02	2.24
Phalanges	0.0	4.3e-07	0.00	1.7e-06	0.01	-	-	-	-	-	-	-	
	0.1	9.0e-04	0.22	7.6e-04	0.20	1.7e-02	3.00	1.7e-02	3.05	3.4e-07	2.25	1.7e-06	2.25
	0.5	2.8e-02	1.12	1.1e-02	0.74	1.7e-02	3.00	1.7e-02	3.04	3.5e-05	2.25	1.1e-04	2.25
	0.7	1.1e-01	1.94	4.3e-02	1.27	1.6e-02	2.99	1.7e-02	2.99	2.3e-03	2.25	6.2e-04	2.24
	0.9	3.3e-01	2.75	2.2e-01	2.26	1.6e-02	2.99	1.7e-02	2.99	7.1e-02	2.26	1.4e-02	2.24
FordA	0.0	2.1e-06	0.02	4.1e-06	0.03	-	-	-	-	-	-	-	
	0.1	7.2e-06	0.04	3.3e-05	0.09	1.7e-02	3.00	1.7e-02	3.02	5.3e-07	2.25	1.7e-06	2.25
	0.5	2.0e-03	0.54	5.1e-03	0.97	1.7e-02	3.02	1.7e-02	3.01	9.4e-05	2.25	8.4e-05	2.25
	0.7	1.9e-02	1.57	2.9e-02	2.06	1.6e-02	2.96	1.6e-02	2.97	3.4e-03	2.25	6.4e-04	2.24
	0.9	1.3e-01	3.52	1.5e-01	3.78	1.7e-02	3.01	1.7e-02	2.99	1.2e-01	2.26	1.6e-02	2.24

4.3 Time Series Generation

To evaluate the utility of learning a prior over the space of implicit functions, we use the set encoder network and the hypernetwork to generate new time series. We do so by projecting time series into the latent vector of the HyperTime network and interpolating the latent vector. This is similar to training an autoencoder and interpolating the latent space, but the output of the decoder of HyperTime are the weights of the SIREN networks. We follow the experimental set up proposed in [1] for the evaluation, where the performance of the synthetic data is evaluated using a predictive score (MAE) that corresponds to the prediction accuracy of an off-the-shelf neural network trained on the synthetic data and tested on the real data. Additionally, to measure the quality of the synthetic data, we use the precision and recall averaged over all time steps, which are then combined into a single F-score. We use the same datasets as before, and we add two datasets that were used in Fourier Flows [1] and TimeGAN [49], Google stocks data and UCI Energy data. We compare our HyperTime model with generating data using PCA, with Fourier Flows and TimeGAN, two state-of-the-art methods for time series generation. Table 3 shows the performance scores for all models and datasets. Additionally, we visualize the generated samples using t-SNE plots 5 where we can see that the generated data from HyperTime exhibits the same patterns as the original data. In the case of Fourier Flows, in the UCR datasets we see that NonInv and Phalanges do not show a good agreement.

The synthesis of time series via principal component analysis is performed in a similar fashion as our HyperTime generation pipeline. We apply PCA to generate a decomposition of time series into a basis of 40 principal components. The coefficients of these components constitute a latent representation for each time series of the dataset, and we can interpolate between embeddings of known time series to synthesize new ones. The main limitation of this procedure, besides its linearity, is that it can only be applied to datasets of equally sampled time series.

Finally, we analyze the importance of the Fourier-based loss \mathcal{L}_{FFT} from equation 3 on the training of HyperTime. In Figure 6-left we display t-SNE visualizations of time series synthesized by HyperTime with and without the use of the FFT loss during training, for two datasets (NonInv and FordA). In both cases, the addition of the \mathcal{L}_{FFT} loss results in an improved matching between ground truth and generated data. However, in the case of FordA, the addition of this loss becomes crucial to guide the learning process. This is also reflected in the numerical evaluations from Table 4, which shows steep improvements in performance for the FordA dataset.

A likely explanation for the difficulty of the network to learn meaningful patterns from the data of this dataset is provided by the right plot in Figure 6. Here we show the standard deviation of the power spectrum for both datasets, as a function of the frequency. The difference in the distributions

Table 3: Performance scores for data generated with HyperTime and for all baselines.

	Crop	NonInv	Phalanges	Energy	Stock
PCA					
<i>MAE</i>	0.050	0.019	0.050	0.007	0.110
<i>F1 Score</i>	0.999	0.999	0.999	0.998	0.999
HyperTime (Ours)					
<i>MAE</i>	0.040	0.005	0.026	0.058	0.013
<i>F1 Score</i>	0.999	0.996	0.998	0.999	0.995
TimeGAN					
<i>MAE</i>	0.048	0.028	0.108	0.056	0.173
<i>F1 Score</i>	0.831	0.914	0.960	0.479	0.938
Fourier Flows					
<i>MAE</i>	0.040	0.018	0.056	0.029	0.008
<i>F1 Score</i>	0.991	0.990	0.992	0.945	0.992

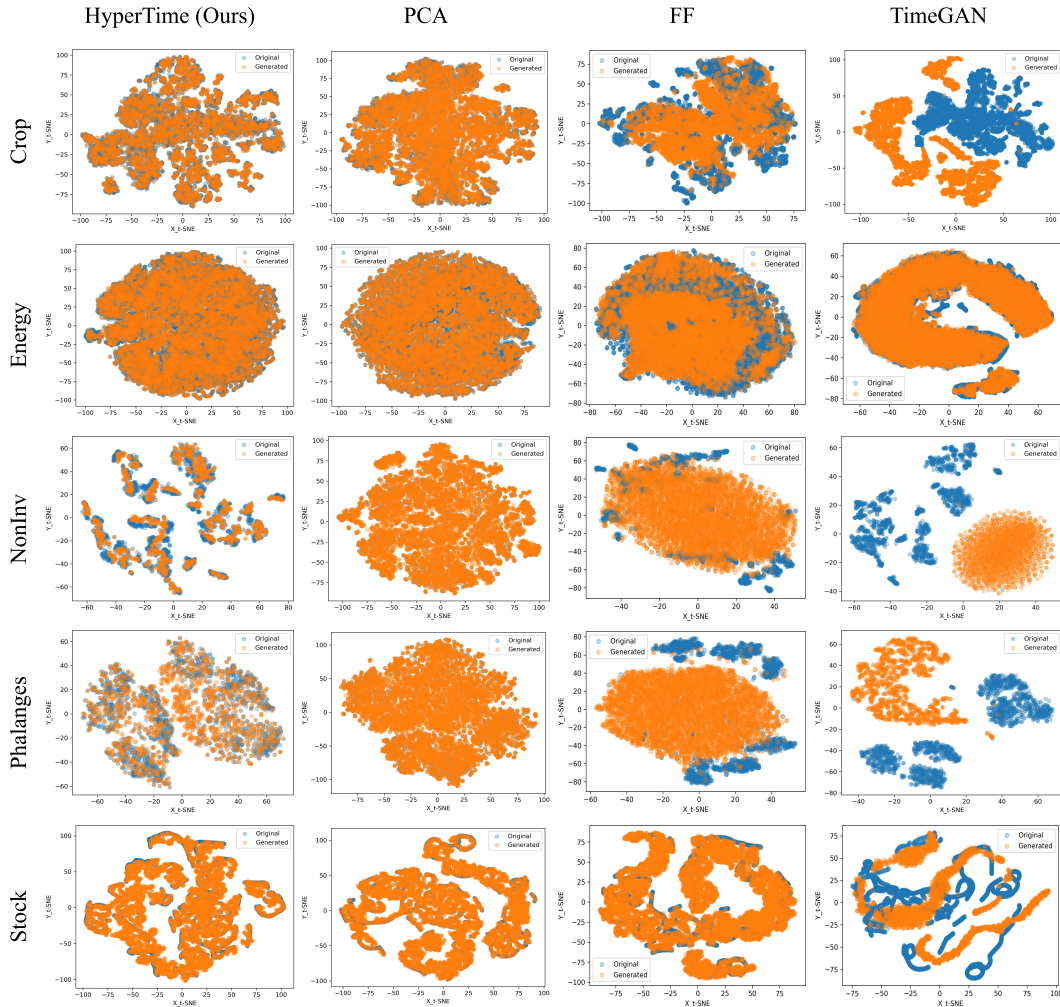


Figure 5: t-SNE visualization on univariate datasets (in rows: Stocks, Energy, Crop, NonInv and Phalanges), using different time series generation methods (in columns: HyperTime, PCA, Fourier Flows and TimeGAN). Blue corresponds to original data and orange to synthetic data.

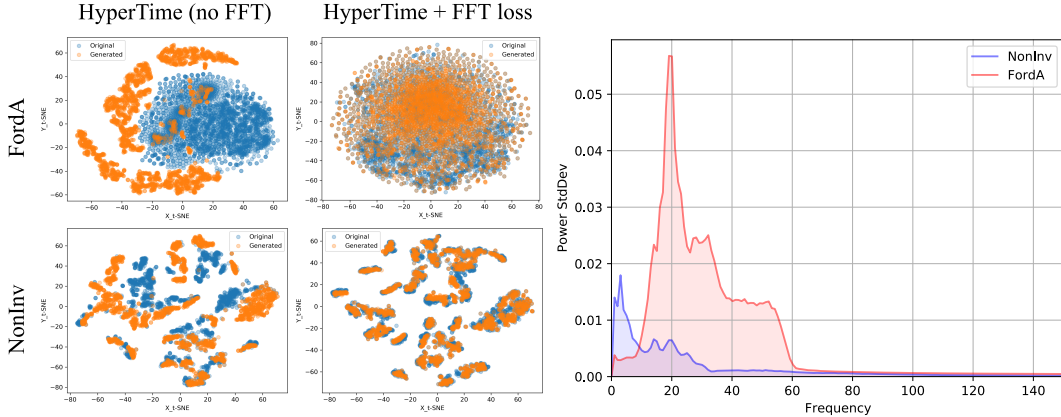


Figure 6: *Left*: t-SNE visualization of ground truth and generated data on two univariate datasets (NonInv and FordA), using HyperNet with and without the Fourier-based loss \mathcal{L}_{FFT} (Eq. 3). *Right*: Standard deviation of the power spectra for the time series of the same two datasets. FordA shows a considerably larger number of variations in the distributions of the power spectra, which explains the difficulty of HyperTime to learn patterns from the data.

indicates that FordA is composed of spectra that present larger variability, while NonInv’s spectra are considerably more clustered. Further research on the characteristics of the datasets that benefit the more from the \mathcal{L}_{FFT} loss should be further investigated, especially focusing on non-stationary time series.

Table 4: Performance scores for data generated with HyperTime, with and without the Fourier-based loss \mathcal{L}_{FFT} , for two datasets (NonInvasiveFetalECGThorax1, FordA).

	NonInv	FordA
HyperTime + FFT loss		
<i>MAE</i>	0.0053	0.0076
<i>F1 Score</i>	0.9962	0.9987
HyperTime (no FFT)		
<i>MAE</i>	0.0058	0.1647
<i>F1 Score</i>	0.9960	0.0167

5 Conclusions

In this paper we explored the use of implicit neural representations for the encoding and analysis of both univariate and multivariate time series data. We compared multiple activation functions, and showed that periodic activation layers outperform traditional activations in terms of reconstruction accuracy and training speed. Additionally, we showed that INRs can be leveraged for data imputation, resulting in good reconstructions of both the original data and its power spectrum, when compared with classical imputation methods. Finally, we presented HyperTime, a hypernetwork architecture to generate synthetic data which enforces not only learning an accurate reconstruction over the learned space of time series, but also preserving the shapes of the power distributions. For this purpose, we introduced a new Fourier-based loss on the training, and showed that for some datasets it becomes crucial to enable the network to find meaningful patterns in the data. We leveraged the latent representations learned by the hypernetwork for the generation of new time-series data, and compared favorably against current state-of-the-art methods for time-series augmentation. Besides reconstruction, imputation and synthesis, we believe that both INRs and HyperTime open the door for a large number of potential applications in time-series, such as upsampling, forecasting and privacy preservation.

Disclaimer This paper was prepared for informational purposes in part by the Artificial Intelligence Research group of JPMorgan Chase & Co and its affiliates (“JP Morgan”), and is not a product of the Research Department of JP Morgan. JP Morgan makes no representation and warranty whatsoever and disclaims all liability, for the completeness, accuracy or reliability of the information contained herein. This document is not intended as investment research or investment advice, or a recommendation, offer or solicitation for the purchase or sale of any security, financial instrument, financial product or service, or to be used in any way for evaluating the merits of participating in any transaction, and shall not constitute a solicitation under any jurisdiction or to any person, if such solicitation under such jurisdiction or to such person would be unlawful.

References

- [1] Ahmed Alaa, Alex James Chan, and Mihaela van der Schaar. Generative time-series modeling with fourier flows. In *International Conference on Learning Representations*, 2021.
- [2] Ali Alqahtani, Mohammed Ali, Xianghua Xie, and Mark W. Jones. Deep time-series clustering: A review. *Electronics*, 10(23), 2021.
- [3] Samuel A. Assefa, Danial Dervovic, Mahmoud Mahfouz, Robert E. Tillman, Prashant Reddy, and Manuela Veloso. Generating synthetic data in finance: Opportunities, challenges and pitfalls. In *Proceedings of the First ACM International Conference on AI in Finance, ICAIF ’20*, New York, NY, USA, 2020. Association for Computing Machinery.
- [4] A. Bagnall, J. Lines, A. Bostrom, J. Large, and E. Keogh. The great time series classification bake off: a review and experimental evaluation of recent algorithmic advances. *Data Mining and Knowledge Discovery*, 31:606–660, 2017.
- [5] Anthony Bagnall, Jason Lines, William Vickers, and Eamonn Keogh. The uea & ucr time series classification repository. www.timeseriesclassification.com. Accessed: 2022-05-10.
- [6] Dimitrios Bellos, Mark Basham, Tony P. Pridmore, and Andrew P. French. A convolutional neural network for fast upsampling of undersampled tomograms in x-ray ct time-series using a representative highly sampled tomogram. *Journal of Synchrotron Radiation*, 26:839 – 853, 2019.
- [7] Nuri Benbarka, Timon Höfer, Hamd ul Moqet Riaz, and Andreas Zell. Seeing implicit neural representations as fourier series. *2022 IEEE/CVF Winter Conference on Applications of Computer Vision (WACV)*, pages 2283–2292, 2022.
- [8] Andrew Brock, Theo Lim, J.M. Ritchie, and Nick Weston. SMASH: One-shot model architecture search through hypernetworks. In *International Conference on Learning Representations*, 2018.
- [9] Wei Cao, Dong Wang, Jian Li, Hao Zhou, Lei Li, and Yitan Li. Brits: Bidirectional recurrent imputation for time series. In S. Bengio, H. Wallach, H. Larochelle, K. Grauman, N. Cesa-Bianchi, and R. Garnett, editors, *Advances in Neural Information Processing Systems*, volume 31. Curran Associates, Inc., 2018.
- [10] Yinbo Chen, Sifei Liu, and Xiaolong Wang. Learning continuous image representation with local implicit image function. In *Proceedings of the IEEE/CVF Conference on Computer Vision and Pattern Recognition*, pages 8628–8638, 2021.
- [11] Kukjin Choi, Jihun Yi, Changhwa Park, and Sungroh Yoon. Deep learning for anomaly detection in time-series data: Review, analysis, and guidelines. *IEEE Access*, 9:120043–120065, 2021.
- [12] Andrea Coletta, Matteo Prata, Michele Conti, Emanuele Mercanti, Novella Bartolini, Aymeric Moulin, Svitlana Vyetenko, and Tucker Balch. Towards realistic market simulations: A generative adversarial networks approach. In *Proceedings of the Second ACM International Conference on AI in Finance, ICAIF ’21*, New York, NY, USA, 2021. Association for Computing Machinery.
- [13] Abhyuday Desai, Cynthia Freeman, Zuhui Wang, and Ian Beaver. Timevae: A variational auto-encoder for multivariate time series generation. *arXiv preprint arXiv:2111.08095*, 2021.
- [14] Chenguang Fang and Chen Wang. Time series data imputation: A survey on deep learning approaches. *ArXiv*, abs/2011.11347, 2020.

- [15] Elizabeth Fons, Paula Dawson, Xiao jun Zeng, John Keane, and Alexandros Iosifidis. Adaptive weighting scheme for automatic time-series data augmentation, 2021.
- [16] David Ha, Andrew M. Dai, and Quoc V. Le. Hypernetworks. In *5th International Conference on Learning Representations, ICLR 2017, Toulon, France, April 24-26, 2017, Conference Track Proceedings*. OpenReview.net, 2017.
- [17] Kyle Hundman, Valentino Constantinou, Christopher Laporte, Ian Colwell, and Tom Soderstrom. Detecting spacecraft anomalies using lstms and nonparametric dynamic thresholding. In *Proceedings of the 24th ACM SIGKDD International Conference on Knowledge Discovery & Data Mining, KDD '18*, page 387–395, New York, NY, USA, 2018. Association for Computing Machinery.
- [18] Hassan Ismail Fawaz, Benjamin Lucas, Germain Forestier, Charlotte Pelletier, Daniel F. Schmidt, Jonathan Weber, Geoffrey I. Webb, Lhassane Idoumghar, Pierre-Alain Muller, and François Petitjean. Inceptiontime: Finding alexnet for time series classification. *Data Mining and Knowledge Discovery*, 2020.
- [19] Brian Kenji Iwana and Seiichi Uchida. An empirical survey of data augmentation for time series classification with neural networks. *PLOS ONE*, 16(7):e0254841, Jul 2021.
- [20] James Jordon, Daniel Jarrett, Evgeny Saveliev, Jinsung Yoon, Paul Elbers, Patrick Thorat, Ari Ercole, Cheng Zhang, Danielle Belgrave, and Mihaela van der Schaar. Hide-and-seek privacy challenge: Synthetic data generation vs. patient re-identification. In Hugo Jair Escalante and Katja Hofmann, editors, *Proceedings of the NeurIPS 2020 Competition and Demonstration Track*, volume 133 of *Proceedings of Machine Learning Research*, pages 206–215. PMLR, 06–12 Dec 2021.
- [21] James Jordon, Jinsung Yoon, and Mihaela van der Schaar. Pate-gan: Generating synthetic data with differential privacy guarantees. In *ICLR*, 2019.
- [22] Bryan Lim and Stefan Zohren. Time-series forecasting with deep learning: a survey. *Philosophical Transactions of the Royal Society A*, 2021.
- [23] Gidi Littwin and Lior Wolf. Deep meta functionals for shape representation. In *IEEE/CVF International Conference on Computer Vision (ICCV)*, pages 1824–1833, 10 2019.
- [24] Yan Liu. Recurrent neural networks for multivariate time series with missing values. *Scientific Reports*, 8(1):6085, 2018.
- [25] Yonghong Luo, Xiangrui Cai, Ying ZHANG, Jun Xu, and Yuan xiaojie. Multivariate time series imputation with generative adversarial networks. In S. Bengio, H. Wallach, H. Larochelle, K. Grauman, N. Cesa-Bianchi, and R. Garnett, editors, *Advances in Neural Information Processing Systems*, volume 31. Curran Associates, Inc., 2018.
- [26] Marius Lysaker. Iterative image restoration combining total variation minimization and a second-order functional. *International Journal of Computer Vision*, 66:5–18, 01 2006.
- [27] Qianli Ma, Jiawei Zheng, Sen Li, and Gary W Cottrell. Learning representations for time series clustering. In H. Wallach, H. Larochelle, A. Beygelzimer, F. d'Alché-Buc, E. Fox, and R. Garnett, editors, *Advances in Neural Information Processing Systems*, volume 32. Curran Associates, Inc., 2019.
- [28] Lars Mescheder, Michael Oechsle, Michael Niemeyer, Sebastian Nowozin, and Andreas Geiger. Occupancy networks: Learning 3d reconstruction in function space. In *Proceedings IEEE Conf. on Computer Vision and Pattern Recognition (CVPR)*, 2019.
- [29] Ben Mildenhall, Pratul P. Srinivasan, Matthew Tancik, Jonathan T. Barron, Ravi Ramamoorthi, and Ren Ng. Nerf: Representing scenes as neural radiance fields for view synthesis. In *ECCV*, 2020.
- [30] Cheolhwan Oh, Seungmin Han, and Jongpil Jeong. Time-series data augmentation based on interpolation. *Procedia Computer Science*, 175:64–71, 2020. The 17th International Conference on Mobile Systems and Pervasive Computing (MobiSPC), The 15th International Conference on Future Networks and Communications (FNC), The 10th International Conference on Sustainable Energy Information Technology.
- [31] Jeong Joon Park, Peter Florence, Julian Straub, Richard Newcombe, and Steven Lovegrove. Deepsdf: Learning continuous signed distance functions for shape representation. In *The IEEE Conference on Computer Vision and Pattern Recognition (CVPR)*, June 2019.

- [32] Mathias Perslev, Michael Jensen, Sune Darkner, Poul Jørgen Jennum, and Christian Igel. U-time: A fully convolutional network for time series segmentation applied to sleep staging. In H. Wallach, H. Larochelle, A. Beygelzimer, F. d'Alché-Buc, E. Fox, and R. Garnett, editors, *Advances in Neural Information Processing Systems*, volume 32. Curran Associates, Inc., 2019.
- [33] Tamar Rott Shaham, Michael Gharbi, Richard Zhang, Eli Shechtman, and Tomer Michaeli. Spatially-adaptive pixelwise networks for fast image translation. In *Computer Vision and Pattern Recognition (CVPR)*, 2021.
- [34] Jacob Russin Russin, Randall O'Reilly, and Yoshua Bengio Bengio. Deep learning needs a prefrontal cortex. In *Bridging AI and Cognitive Science ICLR 2020 Workshop*, 2020.
- [35] Andrei A. Rusu, Dushyant Rao, Jakub Sygnowski, Oriol Vinyals, Razvan Pascanu, Simon Osindero, and Raia Hadsell. Meta-learning with latent embedding optimization. In *International Conference on Learning Representations*, 2019.
- [36] Vincent Sitzmann, Eric R. Chan, Richard Tucker, Noah Snaveley, and Gordon Wetzstein. Metasdf: Meta-learning signed distance functions. In *Proc. NeurIPS*, 2020.
- [37] Vincent Sitzmann, Julien N.P. Martel, Alexander W. Bergman, David B. Lindell, and Gordon Wetzstein. Implicit neural representations with periodic activation functions. In *Proc. NeurIPS*, 2020.
- [38] Vincent Sitzmann, Michael Zollhöfer, and Gordon Wetzstein. Scene representation networks: Continuous 3d-structure-aware neural scene representations. In *Advances in Neural Information Processing Systems*, 2019.
- [39] Ivan Skorokhodov, Savva Ignatyev, and Mohamed Elhoseiny. Adversarial generation of continuous images. In *Proceedings of the IEEE/CVF Conference on Computer Vision and Pattern Recognition (CVPR)*, pages 10753–10764, June 2021.
- [40] Kenneth O. Stanley, David B. D'Ambrosio, and Jason Gauci. A Hypercube-Based Encoding for Evolving Large-Scale Neural Networks. *Artificial Life*, 15(2):185–212, 04 2009.
- [41] Alejandro Sztrajman, Gilles Rainer, Tobias Ritschel, and Tim Weyrich. Neural brdf representation and importance sampling. *Computer Graphics Forum*, 40(6):332–346, 2021.
- [42] Matthew Tancik, Ben Mildenhall, Terrance Wang, Divi Schmidt, Pratul P. Srinivasan, Jonathan T. Barron, and Ren Ng. Learned initializations for optimizing coordinate-based neural representations. In *CVPR*, 2021.
- [43] Matthew Tancik, Pratul P. Srinivasan, Ben Mildenhall, Sara Fridovich-Keil, Nithin Raghavan, Utkarsh Singhal, Ravi Ramamoorthi, Jonathan T. Barron, and Ren Ng. Fourier features let networks learn high frequency functions in low dimensional domains. *NeurIPS*, 2020.
- [44] José F. Torres, Dalil Hadjout, Abderrazak Sebaa, Francisco Martínez-Álvarez, and Alicia Troncoso Lora. Deep learning for time series forecasting: A survey. *Big data*, 2021.
- [45] Johannes von Oswald, Christian Henning, Benjamin F. Grewe, and João Sacramento. Continual learning with hypernetworks. In *International Conference on Learning Representations*, 2020.
- [46] Magnus Wiese, Robert Knobloch, Ralf Korn, and Peter Kretschmer. Quant gans: deep generation of financial time series. *Quantitative Finance*, page 1–22, Apr 2020.
- [47] Haowen Xu, Wenxiao Chen, Nengwen Zhao, Zeyan Li, Jiahao Bu, Zhihan Li, Ying Liu, Youjian Zhao, Dan Pei, Yang Feng, Jie Chen, Zhaogang Wang, and Honglin Qiao. Unsupervised anomaly detection via variational auto-encoder for seasonal kpis in web applications. In *Proceedings of the 2018 World Wide Web Conference, WWW '18*, page 187–196, 2018.
- [48] Jinsung Yoon, Daniel Jarrett, and Mihaela van der Schaar. Time-series generative adversarial networks. In *NeurIPS*, 2019.
- [49] Jinsung Yoon, Daniel Jarrett, and Mihaela van der Schaar. Time-series generative adversarial networks. In *NeurIPS*, 2019.
- [50] Li Zeng, Baifan Zhou, Mohammad Al-Rifai, and Evgeny Kharlamov. Segtime: Precise time series segmentation without sliding window, 2022.
- [51] Chris Zhang, Mengye Ren, and Raquel Urtasun. Graph hypernetworks for neural architecture search. In *International Conference on Learning Representations*, 2019.

- [52] Dominic Zhao, Seijin Kobayashi, João Sacramento, and Johannes von Oswald. Meta-learning via hypernetworks. In *4th Workshop on Meta-Learning at NeurIPS 2020 (MetaLearn 2020)*. NeurIPS, 2020.